Chapter 5
A Method for Reconstructing Surface Spectral Reflectance in Spectral Reproduction Workflow

Ping Yang, Sensen Huang, Wangjian Qiu, Qianyun Ma, Qiang Wang and Hong Song

Abstract In spectral color reproduction workflow, it is of key importance to reconstruct the spectral reflectance of a surface using digital cameras under given luminance and observation conditions. A new approach for solving the problem which is based on neural network and basis vectors is proposed. Compared with other traditional methods, neural network expands the space of unknown function from linear functions to more general nonlinear functions, which gives more accurate estimation of the coefficients and better reflectance reconstruction. Results show that the reflectance of standard Munsell color patch (Matte) can be reconstructed. Compared with linear approximation method, reconstruction of standard Munsell color patch (Matte) using this approach reduces the reconstruction error. Therefore, we conclude that this approach has advantages of higher accuracy, fast implementation, and adaptation, thus can be used in arts reproduction and museum art collection, etc.

Keywords Spectral color reproduction · Basis vectors · Color accuracy

5.1 Introduction

Spectral reflectance is the most complete and accurate approach for color description. It is independent of illumination and observation. Therefore, accurate color replication and object recognition can be achieved based on spectral images, which may find applications in agriculture inspection, museum art collection, medical plastic surgery, and electronic business [1, 2]. But most existing multispectral imaging systems are very complicated in their hardware, having conflicts in

H. Song (✉)
Ocean College, Zhejiang University, Zhejiang, China
e-mail: hongsong@zju.edu.cn

P. Yang · S. Huang · W. Qiu · Q. Ma · Q. Wang
School of Digital Media and Art Design, Hangzhou Dianzi University, Zhejiang, China

Y. Ouyang et al. (eds.), *Advanced Graphic Communications, Packaging Technology and Materials*, Lecture Notes in Electrical Engineering 369,
DOI 10.1007/978-981-10-0072-0_5

their accuracy, structure, and sampling speed. All these impose difficulty for their application in practice [3, 4]. Nowadays, color image acquisition mainly depends on broadband multi-primary color equipments, such as digital camera, scanner, and Web camera. [5, 6]. Thus, how to reconstruct the spectral images based on limited number of multi-channel images is the topic of this paper.

The contribution of our work is that a spectral reflectance reconstruction method has been proposed based on the response from a 4-channel digital color camera. By combining PCA and ANN, the accuracy is improved without introducing extra hardware complex. The paper is organized as follows. Section 5.2 introduces the reconstruction theory and the model. Section 5.3 describes the experimental setup. Section 5.4 explains the experiments and results in detail. Section 5.5 concludes the work.

5.2 Reconstruction Theory

The spectrum range studied in this paper is from 380 to 780 nm, and the reflectance is going to be a 401 dimension vector if the interval is 1 nm. If the interval is 10 nm, still the number of dimension is 41. Though the reflectance dimension is too large, it can be decomposed as a linear combination of the basis vectors by

$$r \approx \sum_{j=1}^{J} a_j \cdot u_j = U_1 \cdot \vec{a} \tag{5.1}$$

where $a_j \in R, \quad j = 1, 2 \ldots J$, which represents linear combination coefficients, $\vec{a}$ represents coefficients vector, and U_1 represents basis vector matrix [7, 8]. So the reflectance R can be written as follows:

$$R = [r_1 r_2 \ldots r_M] \approx U_1 \cdot [a_1 a_2 \ldots a_M] = U_1 \cdot A \tag{5.2}$$

where A represents coefficients vector matrix. A commonly used decomposition method is singular value decomposition (SVD) [9, 15]. By using this method, the reflectance matrix will be decomposed into

$$R = U \cdot \Sigma \cdot V^T = [u_1 \ldots u_N] \cdot \begin{bmatrix} \sigma_1 & & 0 \\ & \cdot & \\ & \cdot & \\ & \cdot & \\ 0 & & \sigma_N \text{ or } \sigma_M \end{bmatrix} \tag{5.3}$$

where U and V^T are both unit orthogonal matrixes and Σ is a diagonal matrix whose diagonal elements are singular values. The diagonal elements satisfy the correlation that $\sigma_1 \geq \sigma_2 \geq \ldots \geq \sigma_J \geq \ldots \geq \sigma_N$ (or σ_M) ≥ 0. And if the first J singular values are

much larger than the subsequent, then the reflectance R matrix can be approximately written as follows:

$$R \approx R_1 = \underbrace{[u_1 \ldots u_N]}_{U_1} \cdot \underbrace{\begin{bmatrix} \sigma_1 & & 0 \\ & \ddots & \\ 0 & & \sigma_N \text{ or } \sigma_M \end{bmatrix} \begin{bmatrix} V_1^T \\ \vdots \\ V_J^T \end{bmatrix}}_{A} \tag{5.4}$$

where $J \ll N$. The contribution rate of the first J singular values can be defined as follows:

$$\eta = \frac{\|R_1\|_2^2}{\|R\|_2^2} \tag{5.5}$$

where $R_1 = U_1 \cdot \mathrm{A}$. Then, some singular values that have the largest contribution to the model will be retained, while the others will be removed, which is the basic idea of PCA [10]. With the help of PCA, the reflectance dimension is greatly reduced. After the dimension is reduced, spectral reflectance can be estimated through either linear model or nonlinear model [10, 11].

Figure 5.1 shows the schematic representation of a two-layer feed-forward neural network consisting of Q tangent hyperbolic neurons in the first layer and M linear neurons in the second layer. The input $S \in R^P$ and output $\hat{a} \in R^M$ satisfy the following relationship:

$$\hat{a} = \mathrm{LW} \cdot \tan \mathrm{h}\,(\mathrm{IW} \cdot \mathrm{S} + \mathrm{b}_1) + \mathrm{b}_2 \tag{5.6}$$

where $\mathrm{IW} \in R^{Q \times P}$ and $\mathrm{LW} \in R^{M \times Q}$ are matrices containing the input and output weights, respectively; $b_1 \in R^Q$ and $b_2 \in R^M$ are biases on the input and output neurons, respectively. IW, LW, b_1, and b_2 can be obtained during the modeling process by optimization algorithm.

From the equation above, it can be seen that a nonlinear function, tangent hyperbolic, is included in the neural network as well as offsets introduced by b_1 and b_2. Thus, the space of the unknown function $F(S)$ is expanded from linear functions

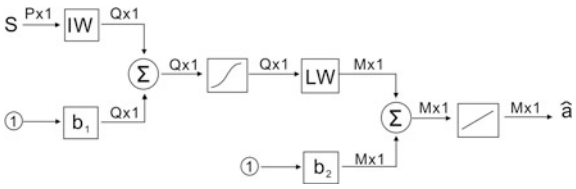

Fig. 5.1 Schematic representation of a two-layer neural network

to more general nonlinear functions. The tangent hyperbolic function has a quite linear behavior when input x is in the range [−0.5, 0.5]. If b_1 and b_2 are both set zero and the matrix IW is chosen such that the product of IW and S is small, then the network can be simplified to be

$$\hat{a} = \mathrm{LW} \cdot \mathrm{IW} \cdot S = M \cdot S \tag{5.7}$$

where matrix $M = \mathrm{LW} \cdot \mathrm{IW}$. Therefore, the linear input–output relationship can be considered as a specific case of this neural network. In this sense, the network should be able to approximate the unknown function $F(S)$ more accurately than any linear function, and it has been reported that a two-layer neural network is able to approximate most nonlinear functions very well [12–15].

5.3 Experimental Setup

The light is generated by a multi-light box (D65 illuminant state), and it emits at an angle of 45 degrees with the vertical direction. Then, it is reflected by the surface of Munsell color cards (Matte, new standard with 1269 cards). After that, the reflected light enters a 4-channel digital color camera and reaches the sensor through the camera's internal imaging systems and filter. Finally, the sensor converts light energy into electrical output to the computer so that the camera response is obtained. The camera response is imported into MATLAB for data processing. The spectral reflectance of the Munsell new standard color cards (matte) is acquired from the online database of University of Joensuu [16], measured by Perkin-Elmer lambda 9 UV/VIS/NIR Spectrophotometer. In 1269 color cards, let the first two in every three cards be used for modeling, and the last one in every three cards be used for testing. During the experiment, in order to ensure the constant lighting conditions and observing conditions, light source and camera are both fixed. And warm up the light box for 10 min before shooting; shooting begins from 5 min after the digital camera is turned on.

5.4 Results

Figure 5.2 shows the measured, nonlinear estimated, and linear estimated spectral reflectance of four color cards chose from 1269 color cards. As can be seen from the figure, the nonlinear estimates curves are very close to the real curves (measured), while the linear estimates curves are not similar to the real curve. Commonly, linear model can be solved by

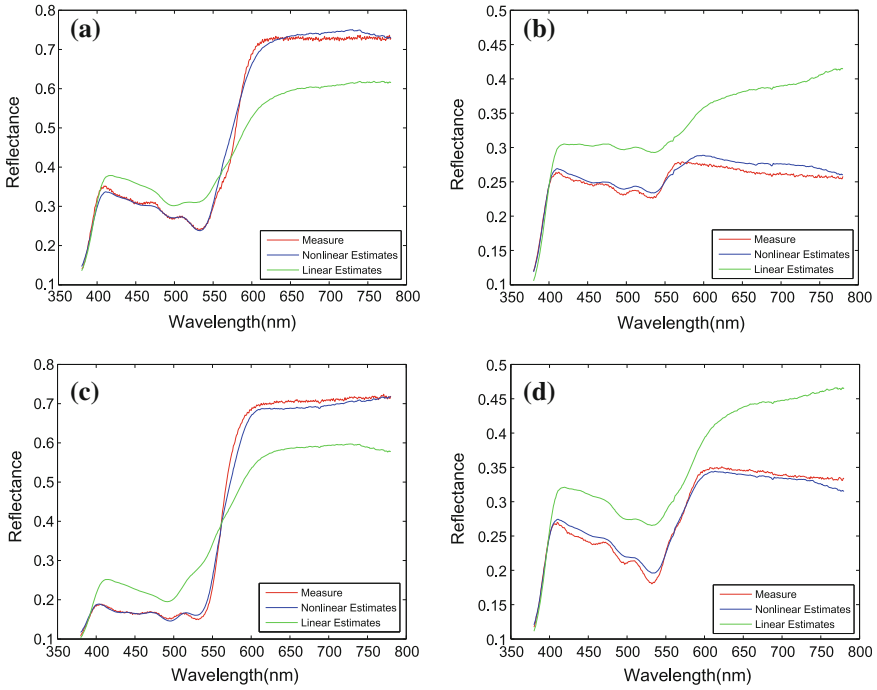

Fig. 5.2 Spectral reflectance of four color cards randomly chose from 1269 color cards **a** spectral reflectance of color card No. 14 **b** spectral reflectance of color card No. 23 **c** spectral reflectance of color card No. 90 **d** spectral reflectance of color card No. 834

$$F = U_1 \cdot A \cdot S^T \cdot (S \cdot S^T)^{-1} \tag{5.8}$$

where U_1 is basis vector matrix, A is coefficient vector matrix, and S is camera response.

And in order to evaluate the accuracy of reconstructed reflectance and to further compare the two models, another eight color cards in training set are used to obtain the $\overline{\text{RMS}}$ and $\overline{\text{STD}}$ error using both nonlinear model and linear model. And the same eight color cards in testing set are used to evaluate the reconstruction accuracy and to see whether the generalization of this kind of neural networks in nonlinear model is good. Table 5.1 shows $\overline{\text{RMS}}$ and $\overline{\text{STD}}$ error statistics of training set and testing set using both nonlinear model and linear model. It can be seen that the $\overline{\text{RMS}}$ and $\overline{\text{STD}}$ error are very close, which means this kind of neural networks used in this paper has good generalization.

Table 5.1 RMS and STD error of eight color cards randomly chose from training set and testing set

No.	Nonlinear method		Linear method	
	Training set	Testing set	Training set	Testing set
$\overline{\text{RMS}}$	0.0696	0.0698	0.0188	0.0203
$\overline{\text{STD}}$	0.0433	0.0435	0.0149	0.0159

5.5 Conclusion

In this paper, we reconstructed the spectrum reflectance based on neural network and basis vectors. Compared with other traditional methods, neural network expands the space of unknown function $F(S)$ from linear functions to more general nonlinear functions, which gives more accurate estimation of the coefficients and better reflectance reconstruction. Results show that the reflectance can be reconstructed successfully. Since the neural network can be implemented by MATLAB neural network toolbox, this method can be easily adapted in many other cases. Therefore, we conclude that this approach has advantages of higher accuracy, easy implementation, and adaptation, thus can be used in many applications.

Acknowledgments The work is supported by Research on Spectral-based Separation relating human perception under multiple light source of Education Department of ZheJiang Province (No. Y201432475), and Research on Technology Integration Standards and Specifications of Cross-media Digital Publishing (No. KYZ223613001), and the Technology Innovation Team of Cross-media Digital Publishing Platform (No. ZX140206320005).

References

1. Hunt, R. W. G. (1987). The reproduction of colour: In photography, printing and television. New York: Fountain Press.
2. Yoichi, M., Yokoyama, Y., Tsumura, T., Haneishi, H., Miyata, K., & Hayashi, J. (1998). Development of multiband color imaging systems for recordings of art paintings. In Proceedings of SPIE (Vol. 3648, pp. 218–225).
3. Imai, F. H., & Berns, R. S. (1999). Spectral estimation using trichromatic digital cameras. In *Proceedings of the International Symposium on Multispectral Imaging and Color Reproduction for Digital Archives* (Vol. 42). Hoboken: Wiley.
4. Saunders, D., & Cupitt, J. (1993). Image processing at the national gallery: The vasari project. *The National Gallery technical bulletin, 14*(1), 72–85.
5. Haneishi, H., Hasegawa, T., Hosoi, A., Yokoyama, Y., Tsumura, N., & Miyake, Y. (2000). System design for accurately estimating the spectral reflectance of art paintings. *Applied Optics, 39*(35), 6621–6632.
6. Ohya, Y., Obi, T., Yamaguchi, M., Ohyama, N., & Komiya, N. (1998). Natural color reproduction of human skin for telemedicine. In *Medical Imaging'98* (pp. 263–270). International Society for Optics and Photonics.
7. Shen, H. L., Cai, P. Q., Shao, S. J., & Xin, J. H. (2007). Reflectance reconstruction for multispectral imaging by adaptive wiener estimation. *Optics Express, 15*(23), 15545–15554.

8. Dupont, D. (2002). Study of the reconstruction of reflectance curves based on tristimulus values: Comparison of methods of optimization. *Color Research & Application, 27*(2), 88–99.
9. Wenhai, Z., Haisong, X., & Yong, W. (2007). Spectral reconstruction of images based on color scanner. *Acta Optica Sinica, 5*, 019.
10. Osorio-Gomez, C. A., Mejıa-Ospino, E., & Guerrero-Bermudez, J. E. (2009). Spectral reflectance curves for multispectral imaging, com-bining different techniques and a neural network. *Revistamexicana de f ́ısica, 55*(2), 120–124.
11. Usui, Shiro, Nakauchi, Shigeki, & Nakano, Masae. (1992). Reconstruction of munsell color space by a five-layer neural network. *Journal of the Optical Society of America, 9*(4), 516–520.
12. Ribes, A., & Schmitt, F. (2003). A fully automatic method for the reconstruction of spectral reflectance curves by using mixture density networks. *Pattern Recognition Letters, 24*(11), 1691–1701.
13. Lopez-Alvarez, M. A., andez-Andres, J. H., Valero, E. M., & Romero, J. (2007). Selecting algorithms, sensors, and linear bases for optimum spectral recovery of skylight. *Journal of the Optical Society of America, 24*(4), 942–956.
14. Laamanen, H. T., Jaeaeskelaeinen, T., & Parkkinen, J. P. (2000). Comparison of PCA and ICA in color recognition. In *Intelligent Systems and Smart Manufacturing* (pp. 367–377). International Society for Optics and Photonics.
15. Hardeberg, J. Y. (2001). Acquisition and reproduction of color images: Colorimetric and multispectral approaches. Boca Raton: Universal Publishers.
16. Joensuu. Spectraldatabase. http://cs.joensuu.fi/∼spectral/databases/download/munsell_spec_matt.htm.Accessed March 10, 2015.